*Clays and Clay Minerals*, Vol. 52, No. 1, 55–65, 2004.

# SERPENTINE-SMECTITE INTERSTRATIFIED MINERALS FROM LOWER SILESIA (SW POLAND)

BORIS A. SAKHAROV[1], ELŻBIETA DUBIŃSKA[2], PAWEŁ BYLINA[3], JAN A. KOZUBOWSKI[4], GRZEGORZ KAPROŃ[2] AND MAŁGORZATA FRONTCZAK-BANIEWICZ[5]

[1] Geological Institute, Russian Academy of Sciences, Pyzhevsky per. 7, 109017 Moscow, Russia
[2] Institute of Geochemistry, Mineralogy and Petrology, Faculty of Geology, Warsaw University, al. Żwirki i Wigury 93, 02-089 Warsaw, Poland
[3] Institute of Geological Sciences, Polish Academy of Sciences, ul. Twarda 51/55, 00-818 Warsaw, Poland
[4] Department of Material Engineering, Warsaw Technical University, ul. Narbutta 85, 02-524 Warsaw, Poland
[5] Medical Research Center, Polish Academy of Sciences, ul. Pawińskiego 5, 02-106 Warsaw, Poland

**Abstract**—Interstratified serpentine-smectite was found in the fine-grained fraction of altered metasomatic contact biotite-schists developed between serpentinite and granite-type rocks (Lower Silesia ophiolite sequence, Poland). Ni-rich serpentine-smectite is R0-interstratified lizardite (0.80)-stevensite (0.15)-vermiculite-like (0.05), with a coherent scattering domain (csd) of 5 layers (mean value). The Mg-rich variety of serpentine-smectite is R1 lizardite (0.80)-stevensite (0.20) with a csd size of 7 layers (mean value). A transmission electron microscope study revealed complex layer relationships, with zones composed of various serpentine-smectite packets having lizardite/smectite ratios of 3:1, 2:1, 1:1, 4:1 and scarce serpentine segregations. In both cases, the serpentine-smectites appear to be late products of alteration of the parent biotite-schist.

Experimental and calculated positions and intensities of reflections of the ethylene glycol-saturated, heated (250ºC, thermal stage), and air-dried samples are in good agreement. Calculated X-ray diffraction patterns for interstratified glycolated and anhydrous serpentine-smectite are included in the Appendix.

**Key Words**—HRTEM, Interstratified Mineral, Laterite, Ni-bearing Layer Silicate, Serpentine-smectite, X-ray Diffraction.

## INTRODUCTION

Interstratified minerals containing 1:1 and 2:1 layers have been found in a variety of geological environments. Examples include interstratified kaolinite-smectite (*e.g.* Sudo and Hayashi, 1956; Sakharov and Drits, 1973; Wiewióra, 1971; Amouric *et al.*, 1995; Amouric and Olives, 1998; Ma and Eggleton, 1999; Righi *et al.*, 1999) and interstratified serpentite-chlorite (*e.g.* Bons and Schryvers, 1989; Jiang *et al.*, 1992; Slack *et al.*, 1992; Banfield *et al.*, 1994; Bailey *et al.*, 1995; Banfield and Bailey, 1996; Dalla Torre *et al.*, 1996; Xu and Veblen, 1996; Schmidt *et al.*, 1999; Schmidt and Livi, 1999; Mata *et al.*, 2001). Dioctahedral interstratified minerals composed of 1:1 and 2:1 layers, *i.e.* kaolinite-smectite, can be common phases as indicated by their occurrence in low-temperature hydrothermal veins from Lower Silesia (Wiewióra, 1971) and in soils developed on basalts in Sardinia (Righi *et al.*, 1999).

Torii *et al.* (1998) and Nagase *et al.* (2000) synthesized interstratified lizardite-smectite, and Gorshkov *et al.* (2002) documented the occurrence of regularly interstratified lizardite-saponite in an altered South African kimberlite. The objective of this paper is to document the occurrence of previously unrecognized irregularly interstratified serpentine-trioctahedral smectite minerals.

* E-mail address of corresponding author:
dubinska@uw.edu.pl
DOI: 10.1346/CCMN.2004.0520107

## GEOLOGICAL SETTING

The interstratified minerals were found in altered metasomatic-thermal contact zones in the magnesite mine at Wiry and an abandoned nickel mine at Szklary (Lower Silesia, Poland, Figure 1). Details on the geology of the contact zones are given in Dubińska (1982), Jelitto *et al.* (1993), and Dubińska *et al.* (1995b, 2000). A number of regular and interstratified layer silicates have been reported from Szklary, including different varieties of serpentine sub-group minerals, chlorite, kerolite-pimelite, Ni-corrensite, clintonite and sepiolite, *etc.* (*e.g.* Ostrowicki, 1965; Wiewióra, 1978; Wiewióra *et al.*, 1982; Wiewióra and Dubińska, 1987; Dubińska *et al.*, 2000).

The sample from Szklary is a soft and brittle, bright green schist that is similar to garnierite as defined by Brindley and Hang (1973). The coarse-grained fraction ($\phi$ >5 μm) of the sample contains a corrensite-like mineral, sceptre-shaped quartz grains, and minor anthophyllite (see Dubińska, 1984 and Dubińska *et al.*, 2000, for details), while the fine-grained fraction ($\phi$ <0.5 μm) contains the previously unidentified interstratified mineral described below. The fine-grained fraction ($\phi$ <0.5 μm) is highly enriched in Ni and contains 18.34 wt.% NiO, while the raw sample contains 7.76 wt.% NiO (Table 1).

The sample from Wiry is a soft and brittle, vermiculite-rich brown schist from the contact ultramafic/granite-type rock. Sakharov *et al.* (2001)

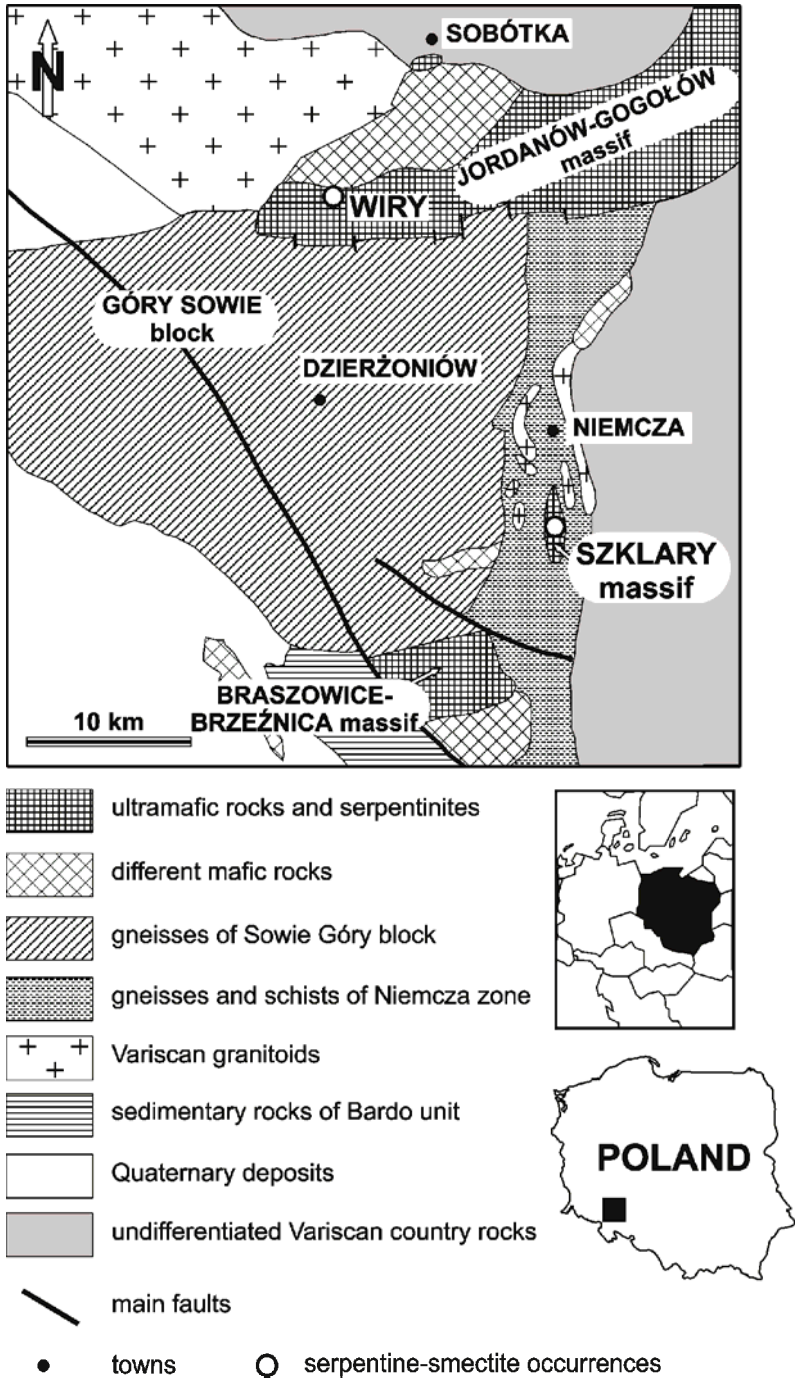


Figure 1. Sketch map of ultramafic massifs adjacent to the eastern and northern borders of the Góry Sowie Mts. Block (SW Poland).

described an unusual vermiculite from the coarse-grained fraction ($\phi$ >0.1 mm) of this sample. The sample also contains chlorite, biotite and various interstratified layer silicates (Dubinska *et al.*, 1995b). The vermiculites formed at the expense of phlogopite and Mg-rich biotite (Dubińska *et al.*, 1995b; Bylina, 1996).

## MATERIAL AND METHODS

Rock samples were disaggregated by soaking the sample in doubly distilled water. Fine-grained fractions were separated using repeated centrifugal sedimentation in doubly distilled water.

X-ray diffraction (XRD) data were obtained on a DRON-1 diffractometer, using CoK$\alpha$ radiation

https://doi.org/10.1346/CCMN.2004.0520107 Published online by Cambridge University Press

Table 1. Chemical composition (wt.%, on anhydrous basis) of rocks and grain fractions containing interstratified serpentine-smectite; wet chemical analysis.

| Sample | Sz50 whole-rock | Sz50 $\phi$ <0.5 μm | Wi34 whole-rock | Wi34 $\phi$ <2 μm |
|---|---|---|---|---|
| $SiO_2$ | 57.49 | 46.55 | 45.93 | 45.77 |
| $TiO_2$ | 0.07 | 0.49 | 0.02 | 0.04 |
| $Al_2O_3$ | 5.34 | 4.94 | 13.34 | 7.25 |
| $Cr_2O_3$ | 0.20 | 0.15 | 0.04 | 0.03 |
| $Fe_2O_{3\ tot.}$ | 5.61 | 4.21 | 5.74 | 9.63 |
| MnO | 0.08 | 0.02 | 0.15 | 0.12 |
| NiO | 7.76 | 18.34 | 0.10 | 0.36 |
| MgO | 22.84 | 25.17 | 32.47 | 36.05 |
| CaO | 0.59 | 0.06 | 0.65 | 0.27 |
| $K_2O$ | 0.01 | 0.06 | 0.63 | 0.03 |
| $Na_2O$ | 0.01 | 0.01 | 0.43 | 0.45 |
| $P_2O_5$ | n.d. | n.d. | 0.50 | n.d. |
| Total | 100.00 | 100.00 | 100.00 | 100.00 |
| LOI | 15.63 | 15.32 | 24.18 | 27.44 |

Sz50 – samples from abandoned nickel mine at Szklary
Wi34 – sample from magnesite mine at Wiry
n.d.: not determined
LOI: loss on ignition

(Fe-filtered), 1.0 and 0.5 mm divergence slits, a 0.25 mm receiving slit, 0.04º2θ steps, and by counting for 5 s per step from 1.5 to 45º2θ. The patterns were collected using the DRONEK software (W. Musiał, unpublished manuscript, 1992). Oriented clay aggregates were prepared on 7 cm long glass slides by the pipette method using 25 mg/cm$^2$ of specimen. The specimens were covered with liquid ethylene glycol and stored in ethylene glycol vapor overnight. The specimens were also heated for 2 h on a custom thermal stage and XRD data were recorded at 250ºC.

Simulated XRD patterns for various structural models were calculated using the ASN program (Drits and Sakharov, 1976). The $z$ atomic coordinates for different layer types were taken from Wicks and Whittaker (1975) and Moore and Reynolds (1997). Instrumental factors, such as sizes of the divergent and receiving slits, specimen size and thickness, and distances between X-ray source, sample and detector were included in calculations according to the recommendations of Drits and Tchoubar (1990). A particle orientation factor, σ*, of 12º (Reynolds, 1986) was also included in the calculations. A lognormal distribution of the csd thickness, as determined by the mean number of layers, and the regression used in the calculations of XRD patterns (Drits *et al.*, 1997) were adopted to obtain the best agreement between calculated and experimental curves. Simulations involved changing the independent parameters for each calculated XRD pattern to obtain close agreement of positions, intensities and profiles of the reflections of the calculated and experimental XRD patterns. The pattern which most closely matched those for both glycolated and heated specimens was selected as the best model of the interstratified structure.

Specimens oriented perpendicular to (001) for high-resolution transmission electron microscope (HRTEM) analysis were embedded with Spurr resin and cut using a diamond knife to obtain specimens of ~50 nm thick. The slices were mounted on copper grid supports, carbon coated and examined in a JEOL JEM 3010 HRTEM. To reduce the effects of damage by the electron beam, the HRTEM images were typically recorded using fast-scan CCD (VHS, 16 frames s$^{-1}$) and slow-scan GATAN CCD (1024 × 1024 pixels) cameras.

## RESULTS AND DISCUSSION

### *Ni-rich serpentine-smectite*

*XRD study.* X-ray diffraction patterns of air-dried, ethylene glycol-solvated, and heated specimens show broad diffraction maxima whose positions and intensities are altered by glycol treatment and heating (Figure 2). The main phase(s) are trioctahedral phyllosilicates as shown by the $d_{060}$ value of 1.532 Å recorded from randomly oriented powder specimens. The peak is tentatively ascribed to a trioctahedral layer silicate. The sample contains a minor amount of talc.

The XRD characteristics of basal reflections of the primary phase(s) did not correspond to any common layer silicate including interstratified varieties, even though we used different procedures and diagrams commonly used for tentative identification of interstratified phases (*e.g.* Méring, 1949; Drits and Sakharov, 1976; Moore and Reynolds, 1997).

We subsequently used a trial and error modeling process to identify the layer silicate in this sample, using data for both the heated and glycolated sample. Two models roughly fit the experimental results:

(1) Interstratified chlorite (0.70)-smectite (0.30) (R = 1, $p_{SS}$ = 0.1) (Figure 3), where R = Reichweite and $p_{SS}$ denotes the independent junction probability of a smectite layer following a smectite layer (according to the notation of Drits and Tchoubar, 1990). The heavy octahedral cations (Ni,Fe) in chlorite were preferentially located in the brucite-like sheet of chlorite to obtain the closest match with peak intensities. The positions and intensities of experimental and calculated diffraction peaks were similar, and the calculated phase, interstratified chlorite-smectite, is well known from different occurrences. However, the calculated pattern of the glycolated sample contains extra peaks (~7.6 Å, 5.18 Å and 2.88 Å) that are not present in the experimental pattern. Moreover, the profile of the 8 Å peak in the calculated X-ray pattern of the heated sample does not fit well with the experimental pattern.

(2) R0 interstratified serpentine (0.80)-smectite (0.20) with a minor admixture of an intergrade-type mineral as described by Walker (1975) (Figure 4); the intergrade mineral contribution to the overall XRD of the studied sample is estimated at 15%. Expandable layers of the interstratified smectite-serpentine show

https://doi.org/10.1346/CCMN.2004.0520107 Published online by Cambridge University Press

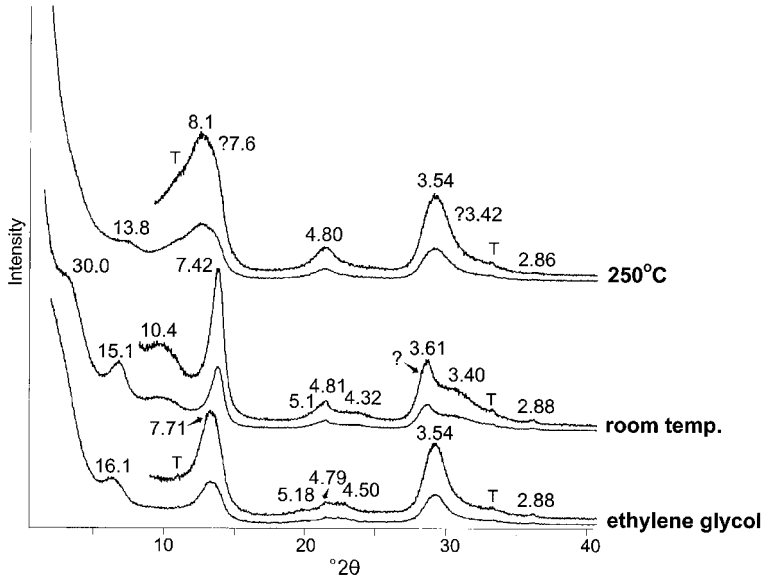


Figure 2. Experimental (observed) XRD patterns of the <0.5 μm fraction of the garnierite sample from Szklary (Sz50); CoKα radiation, oriented specimens; 'ethylene glycol' – ethylene glycol-solvated specimen, 'room temp.' – air-dried specimen, '250ºC' – pattern recorded using a heating stage. T – talc. Spacings in Å.

different behavior during swelling after ethylene glycol treatment and dehydration. Serpentine-smectite treated with ethylene glycol indicates a disordered interstratified structure (R = 0) and contains two types of expandable layers: smectite (A-layer) with a two-layer ethylene glycol complex (16.9 Å, 0.15) and vermiculite-like

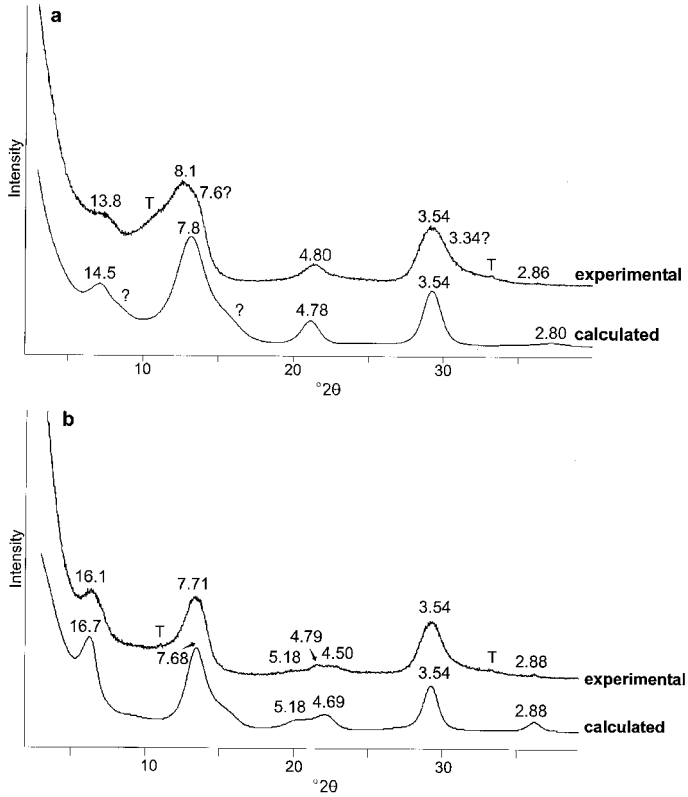


Figure 3. Experimental and calculated XRD patterns of a garnierite sample from Szklary (Sz50, ϕ <0.5 μm); interstratified chlorite (0.70)-smectite (0.30) model, csd 4: (a) XRD patterns of specimen heated to 250ºC. (b) XRD patterns of ethylene glycol-treated specimen. T – talc; for details, see text. CoKα radiation, oriented specimens. Spacings in Å.

https://doi.org/10.1346/CCMN.2004.0520107 Published online by Cambridge University Press

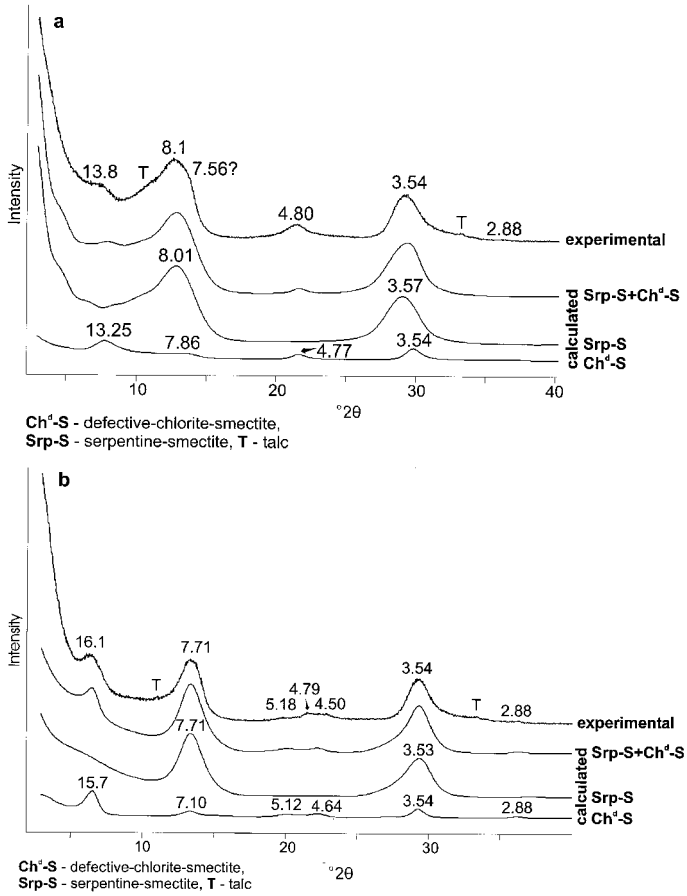


Figure 4. Experimental and calculated XRD patterns of a garnieritic sample from Szklary (Sz50, $\phi$ <0.5 μm); serpentine (0.80)- smectite (0.20) model Srp-S, csd 7; (a) XRD patterns of specimen heated to 250ºC. (b) XRD patterns of ethylene glycol-treated specimen. CoKα radiation, oriented specimens. The sample contains minor intergrade-type mineral, labeled as Ch$^d$-S; the intergrade mineral XRD pattern was calculated using an irregularly (R = 0) interstratified defective chlorite (0.70)-smectite (0.30) model, where the brucite-like sheet was reduced to 65% as compared to the regular chlorite layer. T – talc; for details, see text. Spacings in Å.

(B-layer) with a one-layer ethylene glycol complex (12.9 Å, 0.05). Heated serpentine-smectite shows segregation of 10 Å-smectite pairs ($p_{SS}$ = 0.3, $p_S$ = 0.2, $s_S$ = 0.22, where $s_S$ denotes the degree of segregation after Drits and Tchoubar, 1990). Different swelling of smectite- and vermiculite-like layers produced broad 00*l* values and inhibited identification of smectite segregation on X-ray patterns of the glycolated specimens. Calculated XRD patterns for this structure differ slightly from the observed patterns, suggesting that both models, *i.e.* interstratified chlorite-smectite and serpentine-smectite can be accepted tentatively. However, the fit of experimental and calculated patterns, especially in terms of peak positions for serpentine-smectite, is more appropriate than the chlorite-smectite interstratification model.

*HRTEM study.* The details in the HRTEM images are consistent with the serpentine-smectite model. Lattice fringes of this sample show 7 Å and 10 Å layers (Figure 5), where 10 Å layers represent dehydrated smectite-type layers and 7 Å layers are most abundant. The sequence of layers is generally disordered; moreover, 10 Å:7 Å layer ratios are diverse in different slices. However, regular interstratifications of 10 Å and 7 Å layers (Figure 5c) and zones composed of segregated 10 Å and 7 Å layer domains were also found (Figure 5d). The surface layer can be either 10 Å (Figure 5a and c) or 7 Å (Figure 5b). We did not find 'lateral' transitions between 10 Å and 7 Å layers. The HRTEM study did not reveal an admixture of interstratified chlorite-smectite; it probably reflects a very small chlorite-smectite mineral content.

The serpentine-smectite has high Ni and Mg and low Al contents, as determined by energy-dispersive spectroscopy (EDS). The smectite layers are probably close in composition to a Ni-rich stevensite.

### *Mg-rich serpentine-smectite*

*XRD.* A routine XRD study of the <2 μm fraction of this material revealed major vermiculite, minor biotite, talc and goethite as well as an enigmatic interstratified phase

https://doi.org/10.1346/CCMN.2004.0520107 Published online by Cambridge University Press

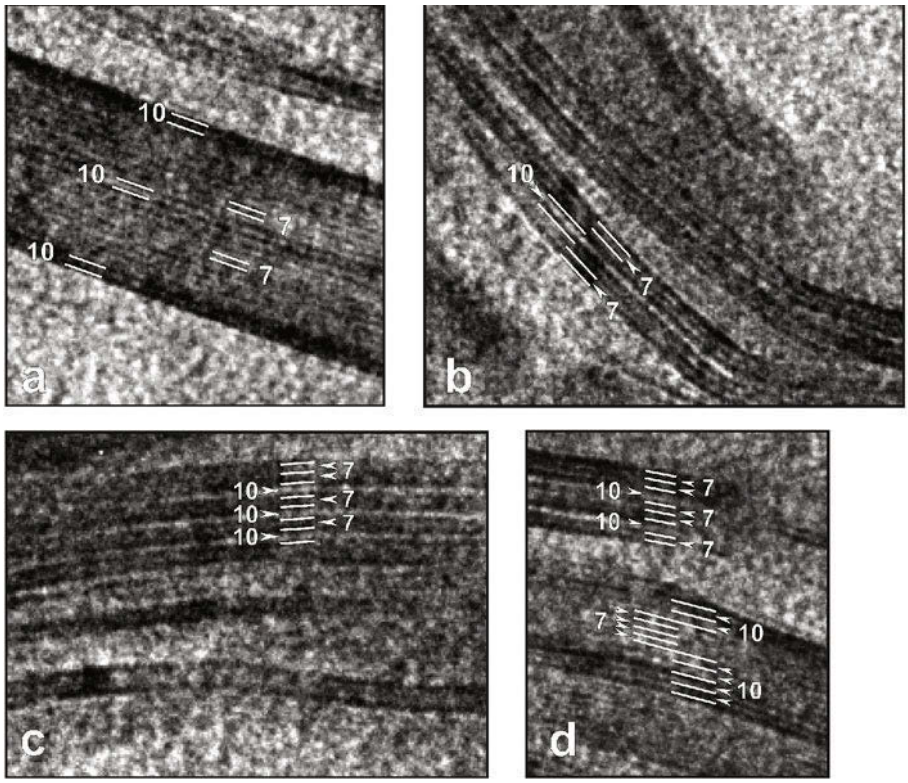


Figure 5. Representative HRTEM images showing the basal lattice fringes of serpentine-smectite particles (sample Sz50, $\phi$ <0.5 μm). (a) Particle composed of 7 Å layer domains separated by single 10 Å layers; 10 Å layers are on both sides of the particle. (b) Thin crystallites composed of 10 Å and 7 Å layers with 7 Å layers as the boundary layers. (c) Quasi-regular sequence of 10 Å and 7 Å layers. (d) Disordered sequence of 10 Å and 7 Å layers.

(Figure 6). The main components of this sample are Mg-rich trioctahedral varieties (Table 1, Dubińska *et al.* 1995b). Previously, the interstratified phase was interpreted as a three-component interstratified chlorite (0.55)-smectite (0.25)-serpentine (0.20) (R = 1, $p_{ChCh}$ = 0.05, $p_{ChS}$ = 0.2, $p_{SCh}$ = 0.4, $p_{SS}$ = 0.6) with Fe preferentially located in the interlayer octahedral sheet of the chlorite layers (Dubińska *et al.* 1995a). However, agreement between the positions of diffraction maxima for the calculated interstratified phase and experimental data was unsatisfactory.

Our results for the Ni-rich serpentine-smectite provide a possible model of the interstratified component present in this sample. Several models of inter-

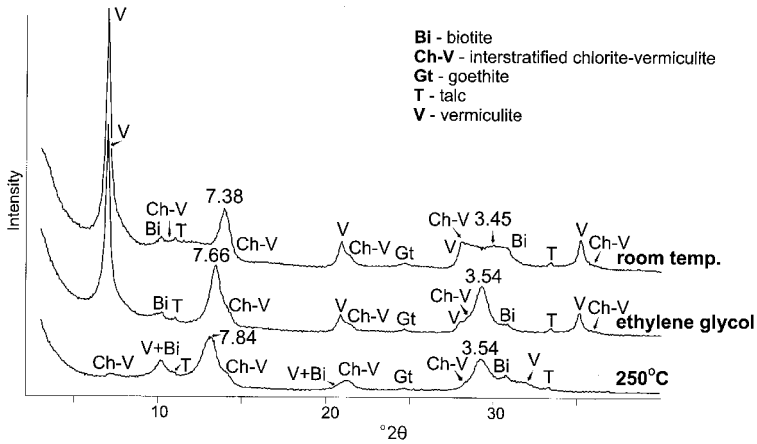


Figure 6. Experimental (observed) XRD patterns of the <2 μm fraction of a vermiculitic sample from Wiry (Wi34); CoKα radiation, oriented specimens; for other explanations see Figure 2. The numbers on the peaks denote apparent *d* spacings (in Å) of diffraction peaks of interstratified serpentine-smectite minerals.

https://doi.org/10.1346/CCMN.2004.0520107 Published online by Cambridge University Press

stratified serpentine-smectite were evaluated for the Mg-rich serpentine-smectite; the best-fit model contains interstratified serpentine (0.80)-smectite (0.20) (R = 1, $p_{SS}$ = 0) and minor irregularly (R = 0) interstratified chlorite (0.65)-vermiculite (0.35) (Figure 7).

*HRTEM study.* This sample was very sensitive to the electron beam, which caused rapid amorphization of the observed crystallites. The studied platelets 'survived' only a few seconds under the electron beam. The HRTEM observations confirmed the abundance of vermiculite platelets (not shown) and the presence of interstratified serpentine-smectite, the latter typically displaying a disordered sequence of serpentine and smectite layers (Figure 8a,b). The serpentine:smectite layer ratio is often close to 4, generally confirming the model proposed on the basis of XRD data. We also observed packets of other serpentine-smectite layer ratios, *e.g.* 3:1, 2:1 and 1:1 as well as packets composed of serpentine layers with single smectite layers (10 Å) and packets rich in 10 Å layers with scarce serpentine.

Packets containing a disordered sequence of 14 Å and 10 Å layers (Figure 8d) confirm the presence of interstratified chlorite-vermiculite as identified using XRD. Moreover, a single packet composed of 14 Å and 7 Å layers was also found during HRTEM investigations (Figure 8c); the lack of diffraction peaks from the serpentine-chlorite interstratified phase obviously reflects its very low content in the studied sample.

## CONCLUSIONS

Structural models and calculated XRD patterns of the Ni- and Mg-rich varieties of interstratified serpentine-

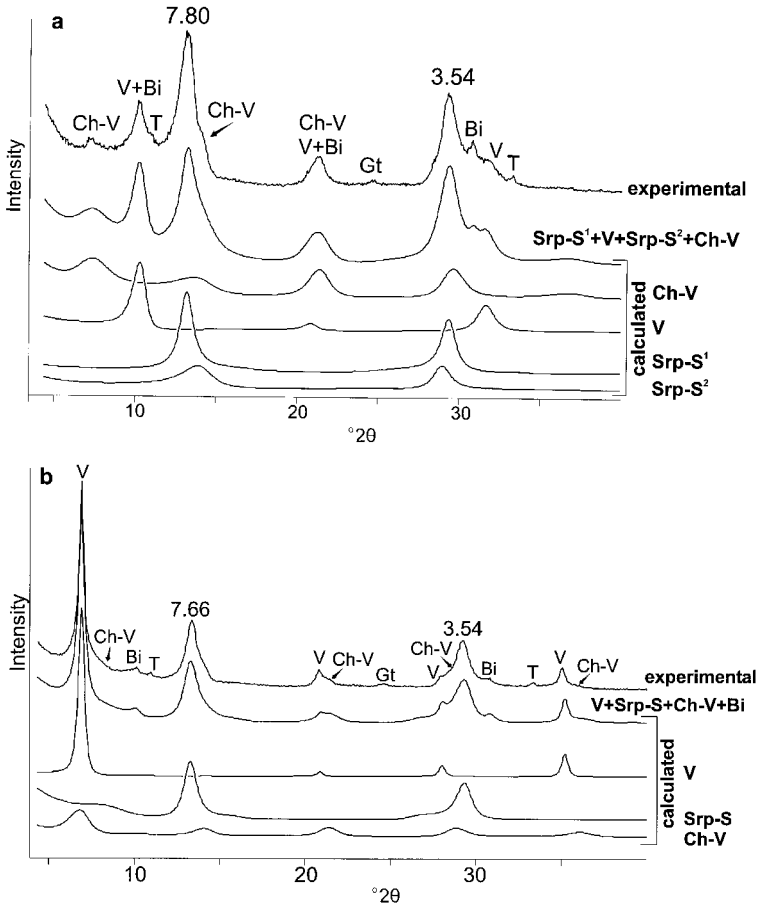


Figure 7. Experimental and calculated XRD patterns of the <2 μm fraction of a vermiculitic sample from Wiry (Wi34, ϕ <2 μm); (a) XRD patterns of specimen heated to 250ºC; calculated pattern refers to the mixture of interstratified serpentine-smectite (major interstratified component) and interstratified chlorite-vermiculite (minor interstratified component), vermiculite and biotite (not shown). The thermally induced collapse of interstratified serpentine-smectite was incomplete and inhomogeneous; two interstratified serpentine-smectite phases were produced: Srp-$S^1$ – serpentine (0.80)-smectite (0.20, anhydrous), Srp-$S^2$ – serpentine (0.85)-smectite (0.10, anhydrous)-smectite (0.05, one-water-layer complex). (b) XRD patterns of an ethylene glycol-treated specimen and calculated pattern of interstratified serpentine (0.80)-smectite (0.20), interstratified chlorite-vermiculite, vermiculite, and biotite. CoKα radiation, oriented specimens; for explanations and details see Figure 6 and text, respectively. Spacings in Å.

https://doi.org/10.1346/CCMN.2004.0520107 Published online by Cambridge University Press

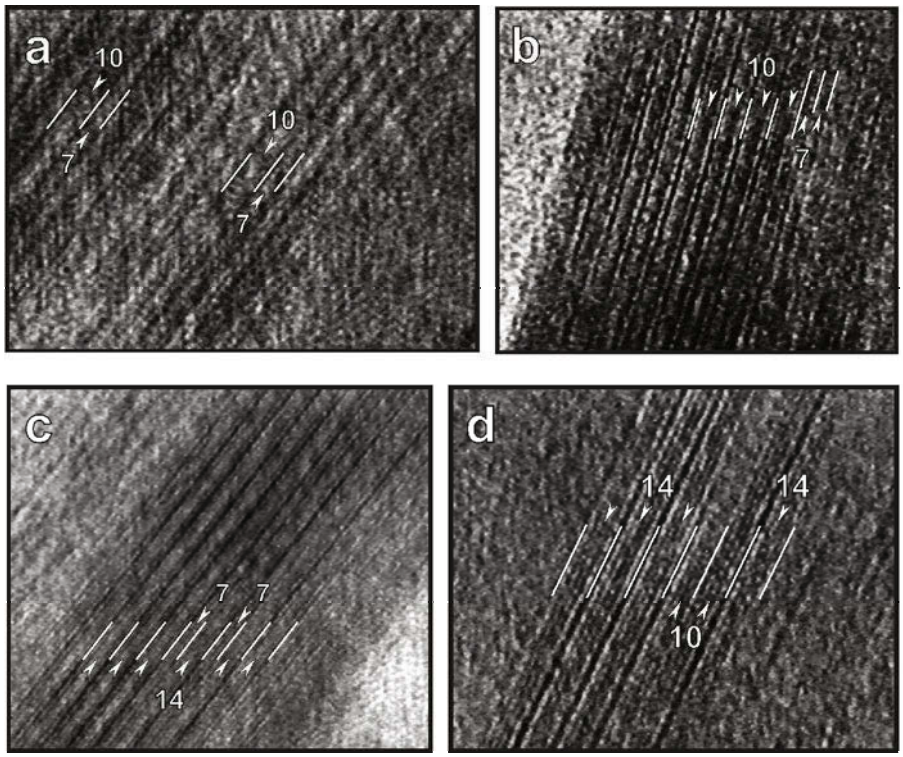


Figure 8. Representative HRTEM images showing the basal lattice fringes of interstratified particles (sample Wi34, $\phi$ <2 μm). (a) and (b) Particles composed of disordered sequences of 10 Å and 7 Å layers. (c) Crystallite composed of 14 Å and 7 Å layers. (d) Crystallites composed of 14 Å and 10 Å layers as an irregular sequence.

smectite from altered ultramafic rocks are consistent with both XRD and HRTEM data. Both Mg-rich and Ni-rich interstratified serpentine-smectites occur in altered biotite-schist developed in contact zones between granite-type apophyses and serpentinite. The Mg-rich interstratified serpentine-smectite occurs in hydrothermally modified contact rocks that record negligible evidence of weathering, although low-temperature (hydrothermal?) alteration is extensive (Dubińska *et al.*, 1995b). The Ni-rich variety occurs in highly weathered rocks from the ultrabasic-felsic rock contact zone (Dubińska, 1984). The Ni enrichment illustrates the well-known mobility of Ni during weathering of ultrabasic rock sequences (*e.g.* Chételat, 1947; Golightly, 1981; Nahon *et al.*, 1982; Colin *et al.*, 1985, 1990), and it suggests low-temperature crystallization of the interstratified Ni-rich serpentine-smectite mineral. An occurrence of sceptre-like quartz in the garnieritic sample (see Dubińska *et al.*, 2000, for details) suggests a significant release of silica that is coincident with the formation of the described interstratified serpentine-smectite at the expense of the precursor 2:1-type layer silicate.

Both the positions and intensities of diffraction peaks of the interstratified serpentine-smectite and their responses to standard clay mineral identification tests strongly resemble the XRD characteristics of intermediate chlorite-vermiculite and chlorite-smectite frequently described from soils (*e.g.* Rich, 1960; Makumbi and Herbillon, 1972; Aurousseau *et al.*, 1983; Carnicelli *et al.*, 1997; Ezzaïm *et al.*, 1999). We do not question the validity of these mineral identifications, but do wish to point out the similarities in XRD patterns of these minerals and of serpentine-smectite. Modifications of relative intensities and asymmetry of the 7 Å and 3 Å reflections on XRD patterns produced by an admixture of interstratified serpentine-smectite in a sample rich in vermiculite or smectite, combined with incomplete dehydration of 2:1 minerals during heating, can also be interpreted as a single intermediate-type structure.

## ACKNOWLEDGMENTS

We are grateful to Ewa Znojek for HRTEM preparation. The authors wish to express their gratitude to David Bish for a critical reading of the manuscript. Constructive comments and suggestions by Dougal McCarty, Peter Ryan and an anonymous reviewer are gratefully acknowledged. The research was supported by Komitet Badań Naukowych (grant 6 PO4D 014 09). Boris A. Sakharov is indebted to the Russian Science Foundation for partial support.

## REFERENCES

Amouric, M. and Olives, J. (1998) Transformation mechanisms and interstratification in conversion of smectite to kaolinite: An HRTEM study. *Clays and Clay Minerals*, **46**, 521–527.

Amouric, M., Parron, C., Casalini, L. and Giresse, P. (1995) A (1:1) 7-Å phase and its transformations in recent sediments:

an HRTEM and AEM study. *Clays and Clay Minerals*, **43**, 446–454.

Aurousseau, P., Curmi, P., Bouille, S. and Charpentier, S. (1983) Les vermiculites hydroxy-alumineux du Massif Armoricain (France). Approches mineralogique, microanalitique et thermodynamique. *Geoderma*, **31**, 17–40.

Bailey, S.W., Banfield, J.F. and Barker, W.W. (1995) Dozyite, a 1:1 regular interstratification of serpentine and chlorite. *American Mineralogist*, **80**, 65–77.

Banfield, J.F. and Bailey, S.W. (1996) Formation of regularly interstratified serpentine-chlorite minerals by tetrahedral inversion in long-period serpentine polytypes. *American Mineralogist*, **81**, 79–91.

Banfield, J.F., Bailey, S.W. and Barker, W.W. (1994) Polysomatism, polytypism, defect microstructures, and reaction mechanisms in regularly and randomly interstratified serpentine and chlorite. *Contributions to Mineralogy and Petrology*, **117**, 137–150.

Bons, A.-J. and Schryvers, D. (1989) High-resolution electron microscopy of stacking irregularities in chlorites from the central Pyrenees. *American Mineralogist*, **74**, 1113–1123.

Brindley, G.W. and Hang, P.T. (1973) The nature of garnierites – I. Structures, chemical compositions and color characteristics. *Clays and Clay Minerals*, **21**, 27–40.

Bylina, P. (1996) Crystallochemistry and genesis of layer silicates from the contact zone between pegmatite and serpentinite from Wiry (Lower Silesia). PhD thesis, Institute of Geological Sciences, Polish Academy of Sciences, Warsaw, Poland, 65 pp. (in Polish).

Carnicelli, S., Mirabella, A., Cecchini, G. and Sanes, G. (1997) Weathering of chlorite to a low-charge expandable mineral in a Spodosol on the Apennine mountains, Italy. *Clays and Clay Minerals*, **45**, 28–41.

Chételat, E. de (1947) La genèse et l'évolution des gisements de nickel de la Nouvelle-Calédonie. *Bulletin de la Societé Géologique de la France*, **17**, 105–160.

Colin, F., Noack, Y., Trescazes, J.-J. and Nahon, D. (1985) L'altération lateritiques debutante des pyroxenites de Jacuba, Niquelandia, Brésil. *Clay Minerals*, **20**, 93–113.

Colin, F., Nahon, D., Trescazes, J.-J. and Melfi, A.J. (1990) Lateritic weathering of pyroxenites at Niquelandia, Goias, Brasil: The supergene behaviour of nickel. *Economic Geology*, **85**, 1010–1023.

Dalla Torre, M., Livi, K.J.T. and Frey, M. (1996) Chlorite textures and compositions from high-pressure/low-temperature metashales and metagraywackes, Franciscan Complex, Diablo Range, California, USA. *European Journal of Mineralogy*, **8**, 825–846.

Drits, V.A. and Sakharov, B.A. (1976) X-ray structural analysis of mixed-layer minerals. *Transactions of the Academy of Sciences U.S.S.R.*, **295**, 1–252 (in Russian).

Drits, V.A. and Tchoubar, C. (1990) *X-ray Diffraction by Lamellar Structures. Theory and Application to Microdivided Silicates and Carbons.* Springer-Verlag, Berlin-Heidelberg-New York-London-Paris-Tokyo-Hong Kong-Barcelona, 371 pp.

Drits, V.A., Środoń J. and Eberl, D.D. (1997) XRD measurement of mean crystallite thickness of illite and illite-smectite: Reappraisal of the Kübler index and the Scherrer equation. *Clays and Clay Minerals*, **45**, 461–475.

Dubińska, E. (1982) Nickel-bearing minerals with chlorite-vermiculite intermediate structure from Szklary near Ząbkowice Śląskie (Lower Silesia). *Archiwum Mineralogiczne*, **38**, 27–51.

Dubińska, E. (1984) Interstratified minerals with chlorite layers from Szklary near Ząbkowice Śląskie (Lower Silesia). *Archiwum Mineralogiczne*, **39**, 5–23.

Dubińska, E., Bylina, P. and Sakharov, B.A. (1995a) Corrensite from Nasławice (Lower Silesia, Poland): Some problems of mineral identification and origin. *Clays and Clay Minerals*, **43**, 630–636.

Dubińska, E., Jelitto, J. and Kozłowski, A. (1995b) Origin and evolution of granite-serpentinite reaction zones at Wiry, Lower Silesia. *Acta Geologica Polonica*, **45**, 41–82.

Dubińska, E., Sakharov, B.A., Kaproń, G., Bylina, P. and Kozubowski, J.A. (2000) Layer silicates from Szklary (Lower Silesia): starting from ocean floor metamorphism to continental chemical weathering. *Geologia Sudetica*, **33**, 85–105.

Ezzaïm, A., Turpault, M.-P. and Ranger, J. (1999) Quantification of weathering processes in an acid brown soil developed from tuff (Beaujolais, France). Part II. Soil formation. *Geoderma*, **87**, 155–177.

Golightly, J.P. (1981) Nickeliferous laterite deposits. *Economic Geology*, 75th Anniversary Vol., 710–735.

Gorshkov, A.I., Zinchuk, N.N., Kotel'nikov, D.D., Shlykov, V.G., Zhukhlistov, A.P., Mokhov, A.V. and Sivtsov, A.V. (2002) A new ordered mixed-layer lizardite-saponite mineral from South African kimberlites. *Doklady Earth Sciences*, **382**, 86–90.

Jelitto, J., Dubińska, E., Wiewióra, A. and Bylina, P. (1993) Layer silicates from serpentinite-pegmatite contact (Wiry, Lower Silesia, Poland). *Clays and Clay Minerals*, **41**, 693–701.

Jiang, W.-T., Peacor, D.R. and Slack, J.F. (1992) Microstructures, mixed-layering and polymorphism of chlorite and berthierine in the Kidd Creek massive sulphide deposit, Ontario. *Clays and Clay Minerals*, **40**, 501–514.

Ma, C. and Eggleton, R. (1999) Surface layer types of kaolinite: a high-resolution transmission electron microscope study. *Clays and Clay Minerals*, **47**, 181–191.

Makumbi, L. and Herbillon, A.J. (1972) Vermiculisation expérimentale d'une chlorite. *Bulletin du Groupe français des Argiles*, **24**, 153–164.

Mata, M.O., Giorgetti, G., Árkai, P. and Peacor, D.R. (2001) Comparison of evolution of trioctahedral chlorite/berthierine/smectite in coeval metabasites and metapelites from diagenetic to epizonal grades. *Clays and Clay Minerals*, **49**, 318–332.

Méring, J. (1949) X-ray diffraction in disordered layer structures. *Acta Crystallographica*, **2**, 371–377.

Moore, D.M. and Reynolds, R.C., Jr. (1997) *X-ray Diffraction and the Identification and Analysis of Clay Minerals*, 2nd edition. Oxford University Press, Oxford-New York, 378 pp.

Nagase, T., Ebina, T., Torii, K., Iwasaki, T., Hayashi, H., Onodera, Y. and Chatterjee, M. (2000) TEM observations of interstratified Ni-serpentine/smectite compounds. *Chemistry Letters*, **4**, 344-345.

Nahon, D., Paquet, H. and Delvigne, J. (1982) Lateritic weathering of ultramafic rocks and the concentration of nickel in the western Ivory Coast. *Economic Geology*, **77**, 1159–1175.

Ostrowicki, B. (1965) Minerały niklu strefy wietrzenia serpentynitów w Szklarach (Dolny Śląsk). *Prace Mineralogiczne PAN*, **1**, 1–92 (in Polish).

Reynolds, R.C. (1986) The Lorentz-polarization factor and preferred orientation in oriented clay aggregates. *Clays and Clay Minerals*, **34**, 359–367.

Rich, C.I. (1960) Aluminum in interlayers of vermiculite. *Soil Science Society of America Proceedings*, **24**, 26–32.

Righi, D., Terrible, F. and Petit, S. (1999) Pedogenic formation of kaolinite-smectite mixed layers in a soil toposequence developed from basaltic parent material in Sardinia (Italy). *Clays and Clay Minerals*, **47**, 505–514.

Sakharov, B.A. and Drits, V.A. (1973) Mixed-layer kaolinite-montmorillonite. A comparison of observed and calculated diffraction patterns. *Clays and Clay Minerals*, **21**, 15–17.

Sakharov, B.A., Dubińska, E., Bylina, P. and Kaproń, G.

(2001) Unusual X-ray characteristics of vermiculite from Wiry, Lower Silesia, Poland. *Clays and Clay Minerals*, **49**, 197–203.

Schmidt, D. and Livi, K.J.T. (1999) HRTEM and SAED investigations of polytypism, stacking disorder, crystal growth, and vacancies in chlorites from subgreenschist facies outcrops. *American Mineralogist*, **84**, 160–170.

Schmidt, D., Livi, K.J.T. and Frey, M. (1999) Reaction progress in chloritic material: an electron microbeam study of the Taveyanne greywacke, Switzerland. *Journal of Metamorphic Geology*, **17**, 229–241.

Slack, J.F., Jiang, W.-T., Peacor, D.R. and Okita, P.P. (1992) Hydrothermal and metamorphic berthierine from the Kidd Creek volcanogenic massive sulphide deposit, Timmins, Ontario. *The Canadian Mineralogist*, **30**, 1127–1142.

Sudo, T. and Hayashi, H. (1956) A randomly interstratified kaolin-montmorillonite in acid clay deposits in Japan. *Nature*, **178**, 1115–1116.

Torii, K., Onodera, Y., Hayashi, H., Nagase, T. and Iwasaki, T. (1998) Hydrothermal synthesis of interstratified lizardite/saponite. *Journal of American Ceramic Society*, **81**, 447–449.

Walker, G.W. (1975) Vermiculites. Pp. 155–189 in: *Soil Components, Volume 2: Inorganic Components* (J.E. Gieseking, editor). Springer, New York-Berlin-Heidelberg.

Wicks, F.J. and Whittaker, E.J.W. (1975) A reappraisal of the structures of the serpentine minerals. *The Canadian Mineralogist*, **13**, 227–243.

Wiewióra, A. (1971) A mixed layer mineral kaolinite-smectite from Lower Silesia, Poland. *Clays and Clay Minerals*, **19**, 415–416.

Wiewióra, A. (1978) Ni-containing mixed-layer silicates from Szklary, Lower Silesia, Poland. *Bulletin BRGM*, **3**, 247–261.

Wiewióra, A. and Dubińska, E. (1987) Origin of minerals with intermediate chlorite-vermiculite structure. *Chemical Geology*, **60**, 185–197.

Wiewióra, A., Dubińska, E. and Iwasińska, I. (1982) Mixed-layering in Ni-containing talc-like minerals from Szklary, Lower Silesia, Poland. *Proceedings of the International*

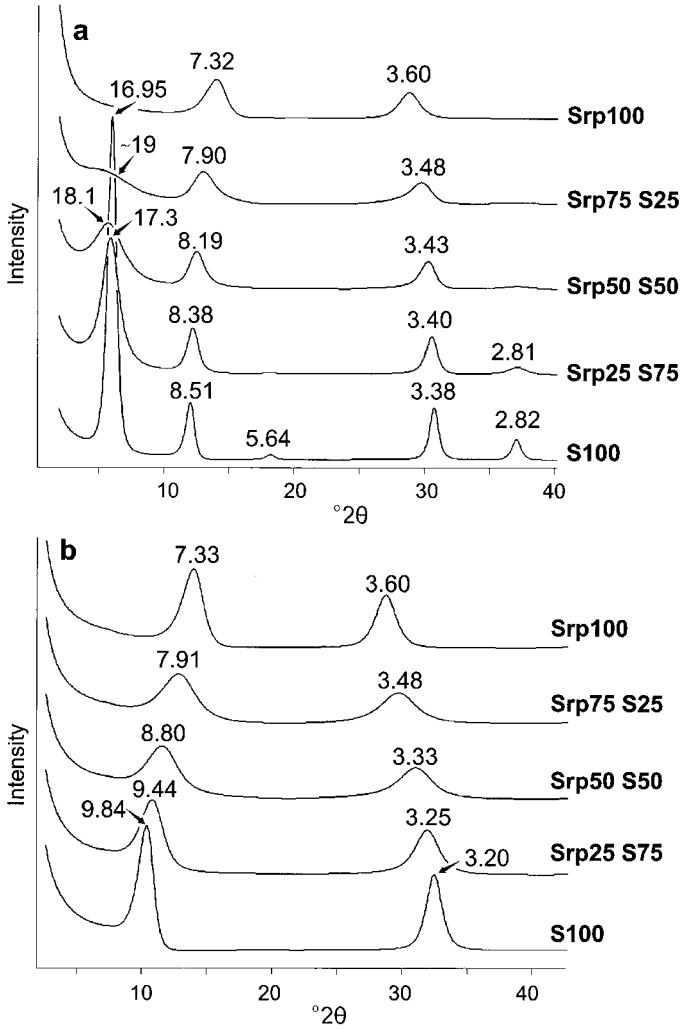


Figure 9. Calculated XRD patterns of interstratified (R = 0) serpentine-smectite ranging from 100% serpentine (Srp100) to 100% smectite (S100); (a) serpentine-smectite (ethylene glycol), (b) serpentine-smectite (anhydrous); CoKα radiation; csd (mean value) = 5. Spacings in Å.

https://doi.org/10.1346/CCMN.2004.0520107 Published online by Cambridge University Press

*Clay Conference 1981*. Elsevier, Amsterdam, pp. 111–125.
Xu, H. and Veblen, D.R. (1996) Interstratification and other reaction microstructures in the chlorite-berthierine series. *Contributions to Mineralogy and Petrology*, **124**, 291–301.

(*Received 6 January 2003; revised 23 September 2003; Ms. 745; A.E. Douglas K. McCarty*)

## APPENDIX

### *XRD identification of serpentine-smectite mixed-layer mineral*

Routine XRD identification of serpentine (kaolinite)-smectite mixed-layer minerals is troublesome and often inconclusive. Kaolinite-smectite interstratified minerals described in the literature typically contain >70% swelling layers (*e.g.* Wiewióra, 1971; Righi *et al.*, 1999). Calculated XRD patterns suggest that identification of mixed-layer serpentine (kaolinite)-smectite in both glycolated and heated specimens is equivocal if the smectite layer content exceeds 50% (Figure 9). Simulated patterns of glycol-treated smectite-rich members of interstratified serpentine-smectite are strikingly similar to those of Fe-rich smectite (for details see Moore and Reynolds, 1997). Incomplete dehydration of smectite layers further complicates identification of mixed-layer serpentine-smectite using heated specimens. Thus the proper identification of mixed-layer serpentine-smectite calls for analyses of several maxima positions as well as unequivocal dehydration of expanding layers during heating.

We have calculated peak-migration curves for serpentine-glycolated smectite and serpentine-collapsed smectite (not shown) for two different crystallite size distributions. The position of the diffraction maximum at ~3.5 Å reveals the serpentine layer content in the interstratification, and the position of the peak at ~8 Å in anhydrous specimens can be used to roughly evaluate the csd. Based on our data and simulations, the XRD patterns of mixtures containing various mixed-layer chlorite-smectite minerals are often indistinguishable from mixed-layer serpentine-smectite, particularly in mixtures. Further HRTEM study is necessary to confirm the identification of a serpentine-smectite mineral.